Numerical and experimental studies of water disinfection in UV reactors

H. Y. Li, H. Osman, C. W. Kang, T. Ba and J. Lou

ABSTRACT

Performance of UV reactors for water disinfection is investigated in this paper. Both experimental and numerical studies are performed on base reactor LP24. Enterobacteria phage MS2 is chosen as the challenge microorganism in the experiments. Experiments are conducted to evaluate the effect of different parameters, i.e. flow rate and UV transmission, on the reactor performance. Simulation is carried out based on the commercial software ANSYS FLUENT with user defined functions (UDFs) implemented. The UDF is programmed to calculate UV dose absorbed by different microorganisms along their flow trajectories. The effect with boundary layer mesh and without boundary layer mesh for LP24 is studied. The results show that the inclusion of boundary layer mesh does not have much effect on the reactor performance in terms of reduction equivalent dose (RED). The numerical results agree well with the experimental measurements, hence validating the numerical model. With this achieved, the numerical model is applied to study other scaled reactors: LP12, LP40, LP60 and LP80. Comparisons show that LP40 has the highest RED and log inactivation among all the reactors while LP80 has the lowest RED and log inactivation.

Key words | log inactivation, numerical simulation, reduction equivalent dose (RED), UV reactor, water disinfection

H. Y. Li (corresponding author)
C. W. Kang
T. Ba
J. Lou
Institute of High Performance Computing (IHPC),
Agency for Science,
Technology and Research (A*STAR),
1 Fusionopolis Way, 16-16 Connexis, Singapore 138632,
Singapore
E-mail: *lih@ihpc.a-star.edu.sg*

H. Osman
Research & Development,
Sembcorp Marine Ltd,
80 Tuas South Boulevard, Singapore 637051,
Singapore

NOMENCLATURE

A	constant (J/m^2)
B	constant (J/m^2)
D	UV dose (J/m^2)
E	fluence rate (W/m^2)
N	number of microorganisms
P	pressure (Pa)
Q	flow rate (m^3/s)
RED	reduction equivalent dose (J/m^2)
t	time (s)
$\vec{u}$	velocity vector (m/s)
UVT	UV transmittance

Greek symbols

ρ	density (kg/m^3)

Subscripts

p	particles
r	reference
*	dimensionless

doi: 10.2166/wst.2019.394

INTRODUCTION

UV radiation is one of the effective ways for both drinking and ballast water disinfection (Hijnen *et al.* 2006; Kong *et al.* 2007). The central ideal of UV radiation for water disinfection is to use UV light to kill the microorganisms or disable them from functioning and reproducing. UV light is known to be able to impair DNA, RNA and cellular structures. When UV light penetrates a microorganism, the energy is absorbed by DNA or RNA, which results in photochemical damage. Such damage inhibits the enzymes used for nucleic acid synthesis. Under such a condition, the damaged DNA or RNA cannot copy during replication. This inactivates the microorganism. The advantage of UV radiation is that it does not introduce or generate any hazardous chemicals or by-products during the procedure. Therefore, it is widely used in water disinfection.

UV dose delivered to an individual microorganism is one of the important factors affecting UV reactor performance. It determines the log reduction of the microorganisms. UV dose

is the product of UV intensity to which the microorganism population is exposed and the exposure time. Different patches of microbial populations absorb different UV dose given their complex flow trajectories under the influence of highly turbulent flow within a reactor of non-uniform UV intensity. Under such a condition, UV reactor performance must be tested under different operating conditions.

Experimental study of a UV reactor for water disinfection involves two stages, i.e. collimated beam test and full-scale test. The collimated beam test is used to get UV dose-response curve of the challenge microorganisms while the full-scale test can be adopted to evaluate UV reactor performance through analysis of log inactivation and reduction equivalent dose (RED). In the experimental test, the measurement of UV dose distribution is critical for the evaluation of UV reactor performance. The measurement of UV dose distribution can be achieved by using the dyed microsphere method developed by Blatchley *et al.* (2006, 2008) for both bench-scale (Blatchley *et al.* 2006) and large-scale (Blatchley *et al.* 2008) UV reactors. The dyed microspheres were used by Zhao *et al.* (2009) to measure the dose distribution in UV reactors with different inlet pipes including straight and elbow shapes. Their results confirm that dyed microspheres can be used as an additional test for UV reactor validation based on the measured UV dose distribution. Shen *et al.* (2009) proposed a Lagrangian actinometry (LA) method based on dyed microspheres to measure UV dose distributions in a UV reactor system. Their tests were conducted using coliphage MS2 as the challenge microorganism. The development of such a method is a breakthrough for the experimental study of UV reactor performance as the LA method can provide accurate prediction of the dose distribution for any microorganism. Gandhi *et al.* (2011, 2012) developed a three-dimensional laser-induced fluorescence method to quantify flow mixing as well as local UV fluence at different locations in a lab-scale UV reactor. Such a method can be easily applied to identify the highest and lowest UV fluence rate so that the UV reactor design can be optimized. The flow around a confined cylinder in a UV reactor was thoroughly investigated by Gandhi *et al.* (2015). Such a fundamental study is quite important for understanding the flow features inside a UV reactor. With good understandings of the flow features, the UV reactor can be designed to work more effectively. Experimental study of a UV reactor for water disinfection, although highly desirable, generally involves sophisticated and high resolution equipment to obtain reliable measurements. Scaled experimental investigation is therefore expensive. Besides, extreme cautiousness is usually demanded if hazardous microorganisms are involved. In view of this, theoretical investigations, in particular numerical study, play an essential complementary role in understanding the disinfection process in UV reactors.

A numerical model for UV disinfection in a reactor includes three components, i.e. fluid flow, microorganism transport and radiation heat transfer. In the numerical simulation, the microorganisms are generally assumed to be solid particles and they are referred to as 'particles' loosely here. Prior to the development of the dyed microorganism method, UV dose distribution is generally predicted through numerical simulations. Lyn *et al.* (1999) proposed a two-dimensional numerical model combined with random walk approach to predict UV dose distribution. Their simulation results compared well with experimental data. Munoz *et al.* (2007) developed a three-dimensional numerical model to predict UV reactor performance. The number of particles required to establish statistically meaningful results was studied. It is revealed from their study that RED is sensitive to the particle numbers. A three-step UV fluence rate and fluid dynamics method was developed by Xu *et al.* (2013) to model the interactions between fluid flow, microorganism particle movement and radiation heat transfer in the UV reactor. Their results showed that the size and shape of the microorganism have negligible effect on UV fluence while water flow rate, reactor size and shape have significant impact on the reactor performance. Further study by the same authors (Xu *et al.* 2015) explored the impacts of lamp arrangement for UV reactor performance. They found that lamp arrangement has complex effects on the log inactivation of the UV reactor under different flow rates. In the evaluation of UV reactor performance, RED is generally used. The calculation of RED requires a cumbersome procedure to switch back and forth between fluence and survival microorganism concentration (Munoz *et al.* 2007). In view of this, Li *et al.* (2016) proposed a new performance indicator of minimum UV dose to replace RED. This new indicator of minimum UV dose is independent of the microorganism dose-response curve and it can be easily obtained from the numerical results. Wright *et al.* (2014) and Gandhi *et al.* (2012) performed numerical simulations based on the Lagrangian method and compared their results against experimental data for UV reactor performance under different parameters. Good agreement was achieved.

Although extensive experimental and numerical studies have been performed with respect to UV reactors for water disinfection, there are no general conclusions for UV reactor performance for different designs and operating conditions. Even if the same UV reactor is used for treating different

microorganisms, the performance could be different. The current work makes continuous efforts to evaluate UV reactors built by SembCorp Marine in Singapore. The main focus here is to study the effects of different parameters on the UV reactor performance based on RED and log inactivation. This is different from the authors' previous work (Li *et al.* 2017) which focuses on the UV dose distributions. In this paper, the effect of boundary layer mesh on the RED is studied. To the best knowledge of the authors, this has not been investigated. Both experiments and numerical simulations are carried out on the base reactor, i.e. LP24. With reasonable agreement achieved between experimental and numerical results, the numerical model is then used to study the performance of other scaled reactors including LP12, LP40, LP60 and LP80. Performance comparisons for these reactors are made in terms of RED and log inactivation.

EXPERIMENTS

UV reactor

Five UV reactors are considered in this study. They are named as LP12, LP24, LP40, LP60 and LP80, respectively. The dimensions of the reactors are scaled based on the number of lamps. LP24 is the bench UV reactor and it is built as a testing bed for experimental study. All the UV reactors have U-shape design. Although different in size and number of lamps fitted, all reactors generally comprise four parts, namely, inlet and outlet pipe, quartz-lamp assemble and two baffle plates. Low-pressure lamps are arranged at different radial locations of the reactor. These lamps are enclosed by cylindrical quartz sleeves protecting the lamps from water. Two baffle plates are used to support the quartz-lamp assembly. These plates are fixed near the center and at outlet boundary of the reactor. A UV sensor is constructed to the ONORM (Sommer *et al.* 2014) standard. It is fixed to measure fluence rate at a point approximately 10 mm from the surface of the quartz in the radial direction.

Experimental setup

Two types of experiments are performed, i.e. bench-scale test using a collimated beam apparatus and full-scale reactor test. The collimated beam test characterizes the relationship between UV dose and log inactivation. It is usually carried out based on a range of doses to generate a UV dose-response curve for a specified challenge microorganism. The full-scale reactor test is used to determine the log inactivation as well as RED. Log inactivation is obtained by measuring the concentrations of the microorganism before and after exposure to UV light in a reactor. With log inactivation obtained, RED can be calculated through the dose-response curve from bench-scale test.

In the tests, Enterobacteria phage MS2 is chosen as the challenge microorganism. Experience showed that the application of MS2 bacteriophages lead to better reproducibility and more consistent results (USEPA 2011). Enterobacteria phage MS2 is a virus, which infects bacteria and it is commonly used as surrogate for enteroviruses that infect water supplies. The corresponding host microorganism of MS2 is *Escherichia coli*; this makes MS2 a harmless challenge microorganism. Also, the UV dose-response of MS2 is very well investigated and MS2 has a very wide application range covering UV doses from 200 J/m^2 to 1,500 J/m^2.

Experimental procedure

Figure 1 shows the experimental test facility. A flow meter and two pressure gauges with analogue outputs are installed at connecting spools at the inlet and outlet of the reactor. A portable UVT (UV transmission) meter is used to calibrate water at specific UVTs. The dose tank is filled with freshwater initially. Sodium thiosulfate is then added and mixed well with the freshwater until the desired UVT measured from the UVT meter is obtained. Water with different UVT is pumped through a centrifugal pump to the UV reactor. The lamps are switched on. The challenge microorganisms are introduced at the upstream of the UV reactor. The bacterial diameter injected in the fluid ranged from 10–50 μm. The fluence rate is measured from the installed UV sensor when it has stabilized. The process is repeated for different UVT and flow rates. The log inactivation was determined by measuring the viable MS2 before entering and after exiting the reactor.

The measurement uncertainties in pressure drop and fluence rate are 4.0% and 3.0%, respectively. The uncertainties of RED originate from the uncertainty of the sensor in the bench-scale test as well as the fitting of the dose-response

Figure 1 | Picture of LP24 reactor.

curve. An overall measurement uncertainty for RED is around 13%.

NUMERICAL SIMULATION

Problem description

The problem considered involves fluid flow, microorganism transport and radiation heat transfer. Water with different UVT carrying suspended microorganisms flows into the reactor. As the lamps are switched on, it emits the light inside the reactor. The microorganisms absorb UV dose along their flow path. Given the non-uniform distribution of the UV intensity and the complex trajectories of the microorganism, the UV dose absorbed by different microorganisms is different. The UV dose distribution is calculated numerically. Figure 2 shows the reactor geometries for LP24, LP12, LP40, LP60 and LP80, respectively.

Governing equations

The governing equations include the Navier–Stokes equation, coupled with an appropriate turbulent model for fluid flow,

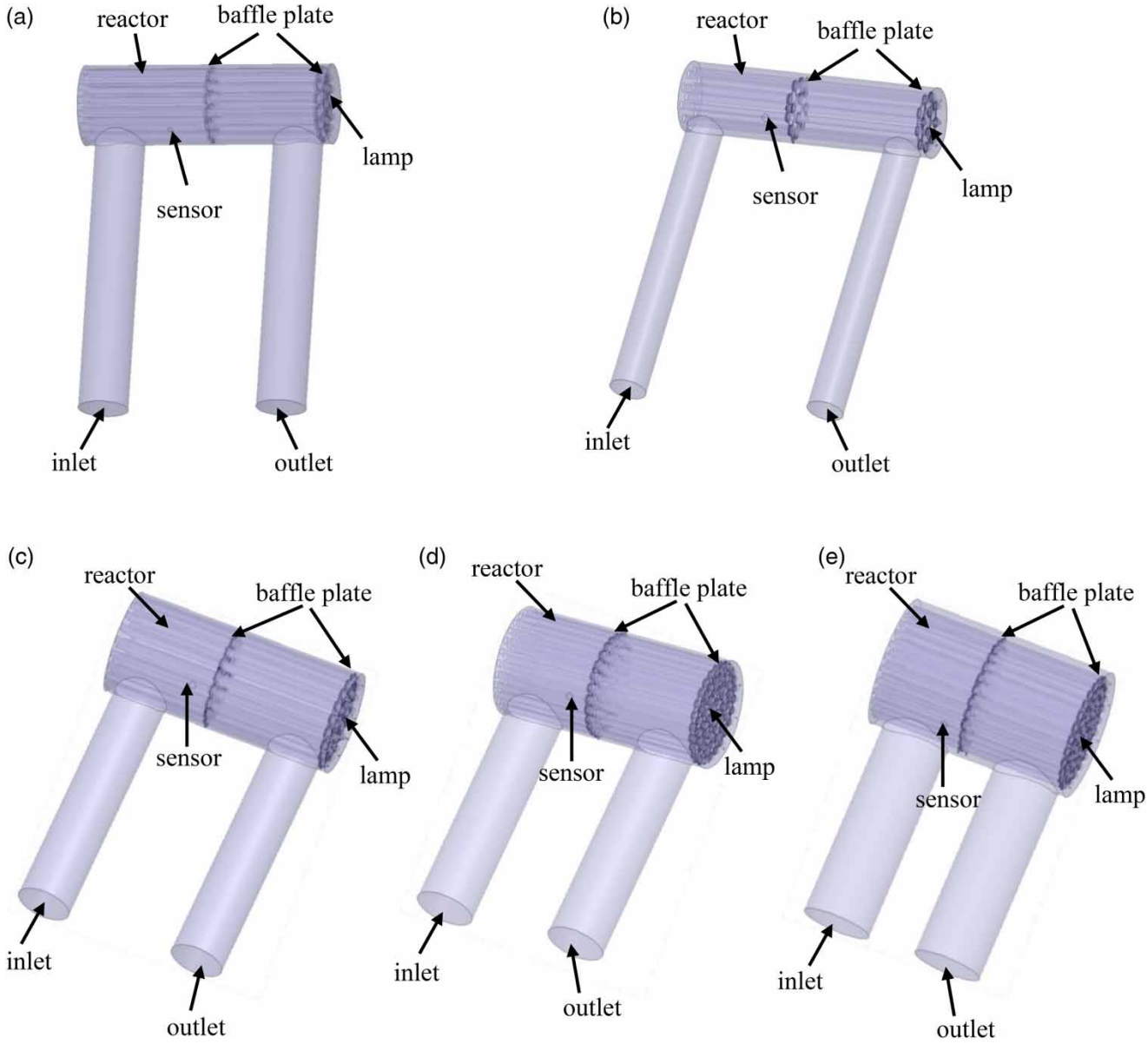

Figure 2 | Simulation geometries for (a) LP24, (b) LP12, (c) LP40, (d) LP60, and (e) LP80.

the energy equation coupled with the discrete ordinates (DO) radiation equation (Raithby & Chui 1990) for radiative heat transfer, and the discrete phase movement equation for microorganism transport (ANSYS 2012). Detailed information of the governing equations as well as the related parameters can be found in the authors' work (Li *et al.* 2017).

UV dose (D) given by Equation (1) is calculated by integrating the fluence rate E over time where fluence rate is obtained by solving the DO radiation equation. The value of UV dose cannot be obtained directly in the simulation. Therefore, a user defined function (UDF) is coded on the ANSYS FLUENT platform. The average value of fluence rates for one particular particle between the consecutive time steps is used to obtain the UV dose in the UDF. The time step is chosen to be 1×10^{-5} s.

$$D = \int_0^t E dt \tag{1}$$

Solution procedure

The simulation procedure is divided into three sequential steps, i.e. solving fluid flow, radiative heat transfer and particle movement. Detailed information can be found in one of the authors' earlier work (Li *et al.* 2017).

RESULTS AND DISCUSSION

UV dose-response curve

The UV dose-response curve reflects the relationship between UV dose and log inactivation. It is determined from bench-scale test using a collimated beam for a specific challenge microorganism. The discrete experimental data of UV dose and log inactivation is plotted and the curve fitted. This curve is then called the UV dose-response curve. Different microorganisms have different UV dose-response curves. Figure 3 shows the UV dose-response curve for the challenge microorganism of MS2 used in the current work. A least-squares fit was performed to obtain the coefficients of A and B in Equation (2).

$$D = A \log\left(\frac{N}{N_0}\right)_i + B\left[\log\left(\frac{N}{N_0}\right)_i\right]^2 \tag{2}$$

where N_0 and N are the number of live microorganisms in the volume of liquid before and after exposure to a UV dose. Log inactivation is expressed as the negative logarithm in base 10 of the survival ratio for N/N_0. A and B are constants which are obtained from the fitting. They are 197.20 and 12.89, respectively. These parameters will be used for RED calculation later. The regression analysis showed a fit with a regression coefficient of $R^2 > 99.98\%$ where R^2 reveals the efficiency and accuracy of the quadratic relationship.

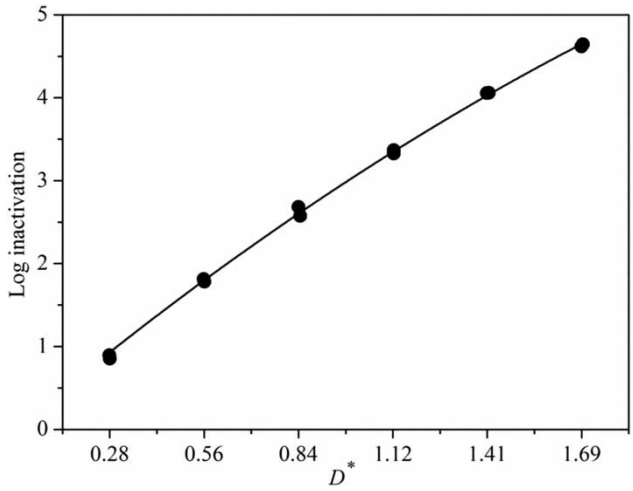

Figure 3 | MS2 dose-response curve.

Mesh and particle number sensitivity study

A mesh and particle number sensitivity study is performed prior to the case study based on LP24. Three different mesh sizes have been employed. The numbers of elements after converting to polyhedral mesh in ANSYS FLUENT are 2.78 million, 4.93 million and 7.83 million, respectively. These are called coarse mesh, medium mesh and fine mesh, respectively. Boundary layers are resolved using wall functions near both the reactor wall and lamp walls to capture the essential flow features. The average y^+ value is set to be 35.

The dimensionless quantities based on the reference values are used for ease of discussions. These reference values include u_r, E_r, Q_r, RED_r and D_r. The subscript r represents reference. u_r and Q_r are the inlet velocity and flow rate based on LP24, respectively. E_r is the fluence rate at UV sensor location at 100% power and UVT55 based on LP24. RED_r is the RED at 100% power and UVT55 based on LP24. D_r is reactor diameter of LP24. Q_r is chosen to be 500 m^3/h as it is the operating flow rate for LP24.

The dimensionless pressure drop is given by:

$$P^* = 2\Delta P/\rho u_r^2 \tag{3}$$

The other dimensionless parameters including u^*, E^* and RED^* are calculated based on the ratio between the numerical results and the corresponding reference values mentioned above for ease of comparison purpose.

The calculation procedure to evaluate RED is given below (Munoz *et al.* 2007):

(1) Calculate N/N_0 based on D obtained from simulation from Equation (1).
(2) Calculate the overall survival ratio of the microorganisms from Equation (4).

$$\frac{N}{N_0} = \sum_{i=0}^{i=n_p} \frac{1}{n_p} \left(\frac{N}{N_0}\right)_i \tag{4}$$

(3) Calculate RED from Equation (5).

$$RED = A \log\left(\frac{N}{N_0}\right) + B\left[\log\left(\frac{N}{N_0}\right)\right]^2 \tag{5}$$

The variations of velocity magnitude perpendicular to the flow direction after the second baffle plate are compared in Figure 4(a). The velocity profile is along a vertical central line at location of 10 mm away from the second baffle plate. It is obvious the velocity profiles between the medium mesh and fine mesh are close to each other. Therefore, the medium mesh is sufficient to capture the flow field. The comparison of UV intensity under different meshes at the same location as the velocity shown above is shown in Figure 4(b). The UV intensity obtained using different meshes overlapped each other. Even the coarse mesh is sufficient to capture the radiation field.

The effect of particle numbers on UV dose is now compared. Three different particle numbers are tested. These are 5,000 particles, 10,000 particles and 20,000 particles, respectively. The comparisons of RED* for different particle numbers for the three meshes are shown in Figure 4(c). The differences for RED* between medium and fine meshes are well within 1% when comparing 10,000 particles and 20,000 particles, respectively. This indicates that the medium mesh is sufficient to capture the particle movement features. The differences for RED* under different number of particles based on medium mesh are 1.7% and 1.2%, respectively, while the differences for RED* under fine mesh for different number of particles are 2.1% and 1.1%, respectively. The differences between 10,000 and 20,000 particles are all well within 2%. Therefore, 10,000 particles are sufficient to get mesh-independent results.

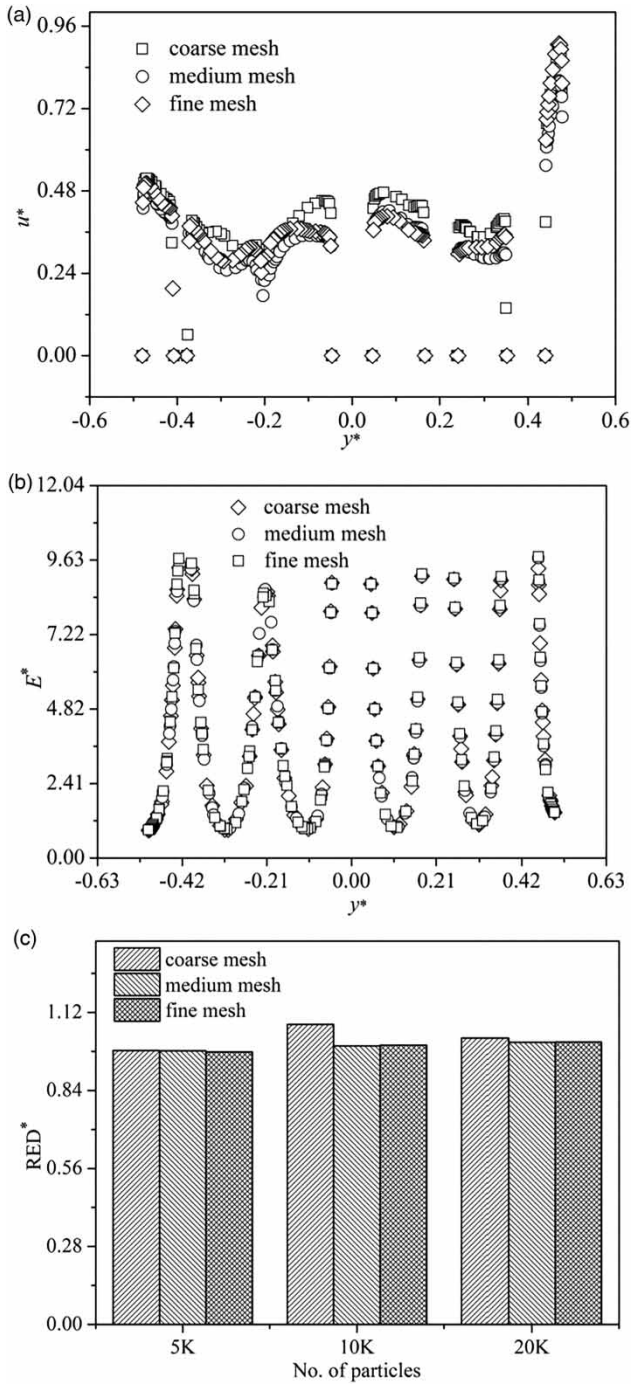

Figure 4 | Mesh independent study for (a) u^*, (b) E^*, and (c) RED* under different particles for different mesh sizes.

Given the fluid flow, radiation and particle study above for different mesh sizes, it is found that the medium mesh with 10,000 particles is sufficient to capture all the essential features involved in the problem. Therefore, the medium mesh size will be used in the simulation for LP24.

Effects of boundary layer mesh for the simulation

The boundary layer refers to the layer of fluid in the vicinity of the wall where the effects of viscosity are significant. The boundary layer usually requires special numerical treatment because of its small thickness. In view of this, boundary layer mesh is generally adopted to capture accurately the main features of flow and heat transfer occurring near the walls. However, the use of boundary layer mesh increases the total mesh in geometry, which subsequently increases the computational time. It is estimated that the computational time for LP80 is more than 100 hours in a Dell workstation of Intel® Xeon® with CPU E5-2650@2.60 GHz and memory of 128 GB. To avoid this, a new mesh is generated and corresponding simulations are performed based on LP24. The mesh size is similar to that used for the medium mesh of LP24. However, no boundary layer mesh is used instead. Figure 5 shows the results comparison for RED* with and without boundary layer mesh under different UVTs. It can be observed that the two curves are overlapping each other, indicating the insignificant effect for boundary layer mesh for simulation of the current problem. Therefore, boundary layer mesh will not be used for other reactors.

Validations

In the current work, experiments are only performed on LP24. Comparisons between experimental and numerical results are made for LP24 at different flow rates and UVTs. Figure 6(a) shows the pressure drop for different flow rates. The solid line is the numerical results while the markers represent experimental data. Generally, the pressure drop increases with the increase of flow rate as expected. Relatively good agreement is achieved between numerical and experimental results.

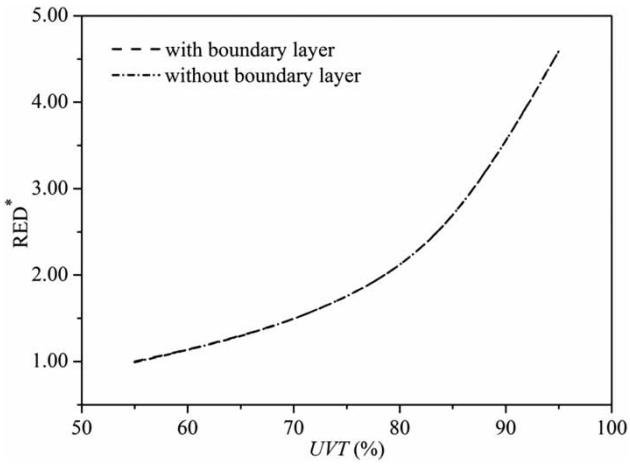

Figure 5 | Comparison of RED* for LP24 with and without boundary layer mesh.

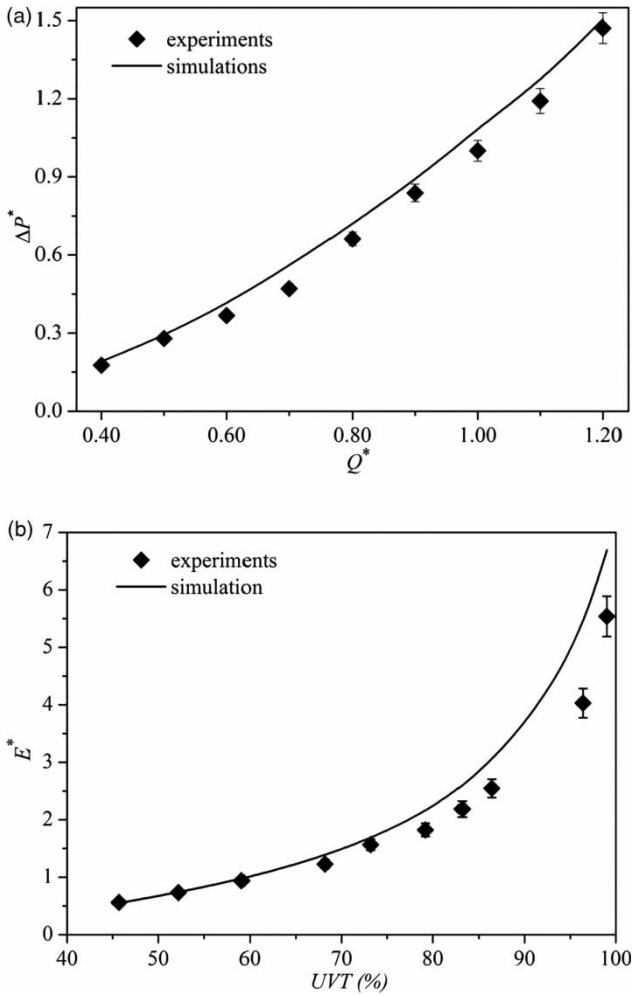

Figure 6 | Comparison of (a) ΔP^*, and (b) E^* between experiments and simulations for LP24.

UV intensity is measured using a UV sensor located on the reactor wall. The average UV intensity at the same location calculated from numerical results is compared against the experimental results. UV transmittance is a measure of UV energy at a particular wavelength or frequency which is actually transmitted through water. The UVT of water depends on the quantity of suspended particles, including organics and colloidal solids. These particles will absorb and scatter UV light, which affects the UV light available for inactivation of microorganisms. Water with high UVT is relatively clear, allowing more UV light to reach the microorganisms. Figure 6(b) shows the variation of

dimensionless UV intensity with UVT. UV intensity increases significantly with the increase of UVT due to the high quality of water with fewer suspended particles. This indicates the importance of water quality for the light to transmit in the UV reactor. Therefore, it is necessary to install a filtration system before the inlet of the UV reactor.

RED is the UV dose calculated from the dose-response curve measured from the collimated beam test. Figure 7 shows the dimensionless RED for different flow rates. RED increases with the increase of UVT for a fixed flow rate. At high UVT, more energy can be transmitted and absorbed by microorganisms. This results in the increase of UV dose and RED. The increase of flow rates reduces the exposure time for microorganisms in the reactor. Therefore, the UV dose absorbed by microorganisms then reduces, leading to a low RED. Generally, the numerical results agree well with experimental data.

Comparisons of different reactors

Comparisons of RED* and log inactivation among different reactors, i.e. LP12, LP24, LP40, LP60 and LP80, under 75% UVT are shown in Figure 8. The inlet flow rates for different reactors are scaled based on the dimensions of the reactors. The flow rates ratio for LP12, LP24, LP40, LP60 and LP80 are 0.5, 1, 1.5, 2 and 3, respectively. Note here the flow rate for LP24 is chosen as the reference value for comparison purpose. The other parameters except for the inlet velocity remain fixed. It is shown in the graphs that LP40 has the highest RED* and log inactivation among all the reactors while LP80 has the lowest RED* and log inactivation. This indicates that, contrary to expectation, the increase of lamp numbers in the reactor does not increase RED* and log inactivation. The determination of RED* and log inactivation is complex as these are dependent on UV intensity and microorganism trajectories. UV intensity depends on many factors such as the number of lamps, lamp locations and lamp power, to name a few. Microorganism trajectories are also affected by the flow conditions and lamp locations. These factors are fully coupled together and cannot be predicted by simple analytical equations or guesswork. Therefore, numerical modelling plays an important role to reveal the dominant factors in affecting the reactor performance.

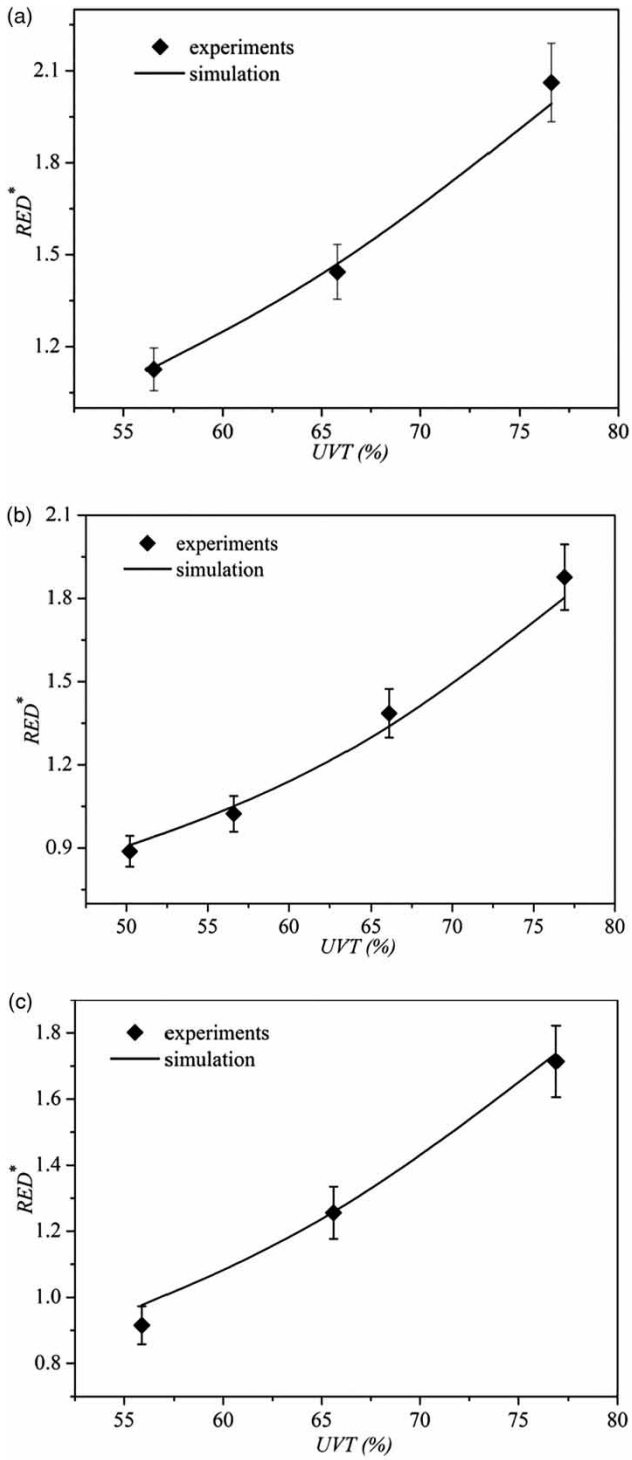

Figure 7 | Comparison of RED* between experimental and simulation results for (a) $Q^* = 0.9$, (b) $Q^* = 1.0$ and (c) $Q^* = 1.1$ based on LP24.

CONCLUSIONS

Performance for water disinfection in five different UV reactors – LP 24, LP12, LP40, LP60 and LP80 – is studied in this paper. Both experimental and numerical modelling is carried out based on LP24. Results show that increase

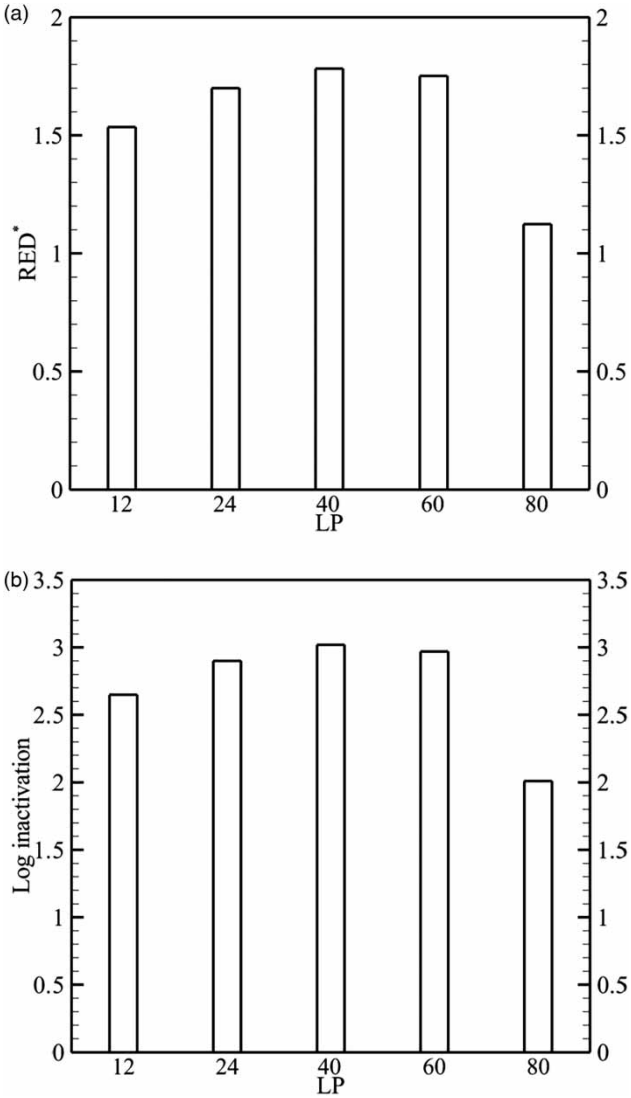

Figure 8 | Comparisons of (a) RED* and (b) log inactivation among different reactors under 75% UVT.

in UVT increases RED while increase in flow rate decreases RED for a given UV reactor. Qualitative comparisons of UV reactor performance in terms of RED as well as log inactivation for the five reactors show that increase of lamp number does not increase RED and log inactivation. LP40 with 40 lamps has the highest RED and log inactivation while LP80 with 80 lamps has the lowest RED and log inactivation among the five reactors. Important engineering implication can be drawn: increasing the number of lamps (i.e. increasing operating cost) does not necessarily increase the reactor performance.

REFERENCES

ANSYS 2012 *ANSYS–FLUENT 12.0, Theory Guide*.

Blatchley III, E. R., Shen, C., Naunovic, Z., Lin, Z. L., Lyn, D. A., Robinson, J. P., Ragheb, K., Grégori, G., Bergstrom, D. E., Fang, S., Guan, Y., Jennings, K. & Gunaratna, N. 2006 Dyed microspheres for quantification of UV dose distributions: photo-chemical reactor characterization by Lagrangian actinometry. *J. Environ. Eng. ASCE* **132** (11), 1390–1403.

Blatchley III, E. R., Shen, C., Scheible, O. K., Robinson, J. P., Ragheb, K., Bergstrom, D. E. & Rokjer, D. 2008 Validation of large-scale, monochromatic UV disinfection systems for drinking water using dyed microspheres. *Water Res.* **42** (3), 677–688.

Gandhi, V., Roberts, P. J., Stoesser, T., Wright, H. & Kim, J. H. 2011 UV reactor flow visualization and mixing quantification using three-dimensional laser-induced fluorescence. *Water Res.* **45** (13), 3855–3862.

Gandhi, V., Roberts, P. J. & Kim, J. H. 2012 Visualizing and quantifying dose distribution in a UV reactor using three-dimensional laser-induced fluorescence. *Environ. Sci. Technol.* **46** (24), 13220–13226.

Gandhi, V., Bryant, D. B., Socolofsky, S. A., Stoesser, T. & Kim, J. H. 2015 Concentration-based decomposition of the flow around a confined cylinder in a UV disinfection reactor. *J. Eng. Mech.* **141** (12), 04015050-1–04015050-12.

Hijnen, W. A. M., Beerendonk, E. F. & Medema, G. J. 2006 Inactivation credit of UV radiation for viruses, bacterial and protozoan (oo)cysts in water: a review. *Water Res.* **40** (1), 3–22.

Kong, X. P., Zhu, Y. M., Zhang, M. X. & Sun, X. J. 2007 Simulated experiment on minimizing the presence *Chlorella* and bacteria in ballast water by combination of micro-hole filtration and UV radiation. *J. Adv. Oxid. Technol.* **10** (1), 186–188.

Li, W. T., Li, M. K., Bolton, J. R. & Qiang, Z. M. 2016 Configuration optimization of UV reactors for water disinfection with computational fluid dynamics: feasibility of using particle minimum UV dose as a performance indicator. *Chem. Eng. J.* **306**, 1–8.

Li, H. Y., Osman, H., Kang, C. W. & Ba, T. 2017 Numerical and experimental investigation of UV disinfection for water treatment. *Appl. Therm. Eng.* **111**, 280–291.

Lyn, D. A., Chiu, K. & Blatchley III, E. R. 1999 Numerical modeling of flow and disinfection in UV disinfection channels. *J. Environ. Eng.* **125** (1), 17–26.

Munoz, A., Craik, S. & Kresta, S. 2007 Computational fluid dynamics for predicting performance of ultraviolet disinfection-sensitivity to particle tracking inputs. *J. Environ. Eng. Sci.* **6** (3), 285–301.

Raithby, G. D. & Chui, E. H. 1990 A finite-volume method for predicting a radiant heat transfer in enclosures with participating media. *J. Heat Transfer* **112** (2), 415–423.

Shen, C., Scheible, O. K., Chan, P., Mofidi, A., Yun, T. I., Lee, C. C. & Blatchley III, E. R. 2009 Validation of medium-pressure UV disinfection reactors by Lagrangian actinometry using dyed microspheres. *Water Res.* **43** (5), 1370–1380.

Sommer, R., Cabaj, A., Haider, T. & Hirschmann, G. 2014 UV drinking water disinfection – requirements, testing and surveillance: exemplified by the Austrian National Standards M 5873–1 and M 5873–2. *IUVA News* 6.

USEPA (US Environmental Protection Agency) 2011 *Challenge Organisms for Inactivation of Viruses by Ultraviolet Treatment*. Available from: http://www.waterrf.org/PublicReportLibrary/3105.pdf.

Wright, H., Gandhi, V., Salveson, A. & Wicklein, E. 2014 CFD-based UV dose prediction tool for wastewater reuse applications. In: *Proceedings of the Water Environment Federation*, 27 September–1 October, New Orleans, LA, USA.

Xu, C., Zhao, X. S. & Rangaiah, G. P. 2013 Performance analysis of ultraviolet water disinfection reactors using computational fluid dynamics simulation. *Chem. Eng. J.* **221**, 398–406.

Xu, C., Rangaiah, G. P. & Zhao, X. S. 2015 A computational study of the effect of lamp arrangements on the performance of ultraviolet water disinfection reactors. *Chem. Eng. Sci.* **122**, 299–306.

Zhao, X., Alpert, S. M. & Ducoste, J. J. 2009 Assessing the impact of upstream hydraulics on the dose distribution of ultraviolet reactors using fluorescence microspheres and computational fluid dynamics. *Environ. Eng. Sci.* **26** (5), 947–959.

First received 24 May 2019; accepted in revised form 18 November 2019. Available online 28 November 2019